Title

Error probability performance for W-CDMA systems with multiple transmit and receive antennas in correlated Nakagami fading channels

Journal

IEEE Transactions on Vehicular Technology, 51(6)

ISSN

0018-9545

Authors

Luo, J X
Zeidler, J R
Proakis, J G

Publication Date

2002-11-01

Peer reviewed

Error Probability Performance for W-CDMA Systems With Multiple Transmit and Receive Antennas in Correlated Nakagami Fading Channels

Jianxia Luo, *Member, IEEE*, James R. Zeidler, *Fellow, IEEE*, and John G. Proakis, *Life Fellow, IEEE*

***Abstract*—The bit error rate (BER) performance of a two-dimensional (2-D) RAKE receiver, in combination with transmit diversity on the downlink of a wide-band CDMA (W-CDMA) system, is presented. The analyses assume correlated fading between receive antenna array elements, and an arbitrary number of independent but nonidentical resolvable multipaths combined by the RAKE receiver in the general Nakagami-m fading channel framework. The impact of the array configuration (e.g., the number of transmit antennas and receive antennas, the antenna element separation) and the operating environment parameters (such as the fading severity, angular spread and path delay profile) on the overall space-path diversity gain can be directly evaluated. In addition, the exact pairwise error probability of a convolutional coded system is obtained, and the coding gain of a space-path diversity receiver is quantified.**

***Index Terms*—Convolutional coding, correlated Nakagami fading, multiple-input–multiple-output (MIMO) systems, pairwise error probability, space-path diversity, two-dimensional (2-D) RAKE receiver.**

I. Introduction

MULTIPLE-INPUT–MULTIPLE-OUTPUT (MIMO) systems are a natural extension of developments in antenna array communications. The array gain and spatial diversity obtained by utilizing multiple receive antennas have been thoroughly investigated both theoretically [2]–[7] and experimentally, but the advantages of MIMO communications which exploit the physical channels between many transmit and receive antennas, denoted as (M_T, M_R), can provide further performance improvements. It has been shown theoretically [8], [9] that, as $M = \min(M_T, M_R)$ grows toward infinity, for a given fixed average transmitter power, if the fades between pairs of transmit-receive antenna elements are independent and identically Rayleigh, the average channel capacity divided by M approaches a nonzero constant determined by the average signal-to-noise ratio. This implies that multiple antenna systems have potentially important applications in broad-band wireless communications. Also, simulation studies [10], [12] and experiment measurements [11] have been completed for a variety of propagation conditions, in order to quantify the realistic performance gains with multiple antenna elements (MAE). In addition to the capacity increase, Bjerke, *et al.* [13] presented the BER performance of maximal-ratio combining (MRC) or selection receive antenna combining, in combination with open-loop and closed-loop transmit diversity, for a (2, 2) MIMO W-CDMA systems in Rayleigh fading.

Forward error correction (FEC) coding provides an alternative method to improve the performance of communications on wireless fading channels. For coding to be effective, bit errors in each code word should be independent. To render the channel memoryless (i.e., to randomize bursty errors which are often encountered in fading environments), perfect bit interleaving is usually assumed. In this paper, we investigate the performance of combined diversity and convolutional coding strategies. Performance analysis of coded CDMA systems in Rayleigh fading appeared in [14]–[20]. In particular, Diaz and Agusti [14] presented closed form analytical BER expressions achieved in a coherent BPSK DS-CDMA system for any power-delay profile and for either selection combining or MRC in independent Rayleigh fading assuming distinct path SNR. For convolutionally coded transmission, the relation of their bound on BER to the channel cutoff rate [15] was also given. The concatenation of Reed–Solomon and convolutional codes in asynchronous CDMA with selection antenna diversity is studied in [17], and the tradeoff analysis among various system parameters under a fixed bandwidth expansion and concatenated code constraint requirement is provided. The effect of the positive correlation between the Rayleigh fading channel amplitudes due to imperfect power control and nonideal block interleaver, when a low-rate convolutional code is applied, is quantified in [20].

In mobile radio systems, the transmitted signal is attenuated, reflected, and refracted by many obstacles along the paths between the transmitter and the receiver. Early propagation experiments [1] indicate the Nakagami-m distribution is one of the most versatile models to describe the fading statistics. The Nakagami-m distribution includes the Rayleigh distribution as a special case for $m = 1$; it can also accurately approximate the Rician fading when $m > 1$, with one-to-one mapping between the fading parameter m and the Rician K-factor.

Manuscript received August 1, 2001; revised March 26, 2002. The material in this paper was presented in part at the IEEE Globecom Conference, San Antonio, TX, November 2001 and at the IEEE International Conference on Communications, New York, NY, April 2002.

J. Luo was with Department of Electrical and Computer Engineering, University of California, San Diego, La Jolla, CA 92093-0407 USA. She is now with Hughes Network System, Inc., San Diego, CA 92121 USA (e-mail: jluo@hns.com).

J. R. Zeidler is with the Department of Electrical and Computer Engineering, University of California, San Diego, CA 92093-0407 USA, and also with the Space and Naval Warfare Systems Center, San Diego, CA 92152-5001 USA (e-mail: zeidler@ece.ucsd.edu)

J. G. Proakis is with the Department of Electrical and Computer Engineering, University of California, San Diego, CA 92093-0407 USA, and is also Professor Emeritus with the Department of Electrical and Computer Engineering, Northeastern University, Boston, MA 02115 USA (e-mail:proakis@ neu.edu).

Digital Object Identifier 10.1109/TVT.2002.804861

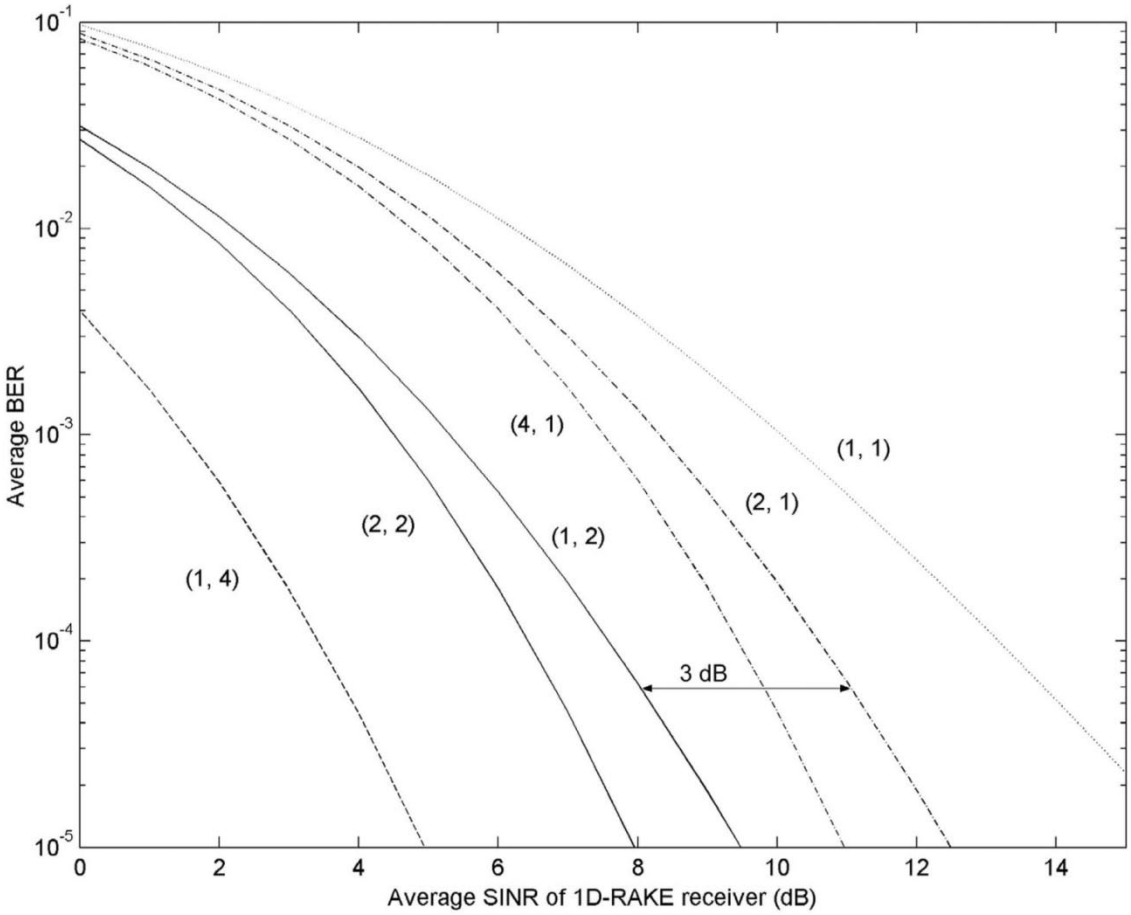

Fig. 1. Performance comparison of various MAE systems, independent receive signals, $n\bar{m} = 1$ Rayleigh fading channel, with constant MIP.

BER performance and capacity assessment of a DS-CDMA system with RAKE reception and convolutional coding under frequency-selective Nakagami fading are given in [22], based on hard-decision Viterbi decoding. In [23], tight upper bounds on the BER of convolutional codes with soft-decision decoding over independent Nakagami, Rayleigh, and Rician fading multipath channels are evaluated. However, the analysis does not consider space diversity and the bound for the Nakagami fading case is obtained under the following constraint: the ratio of the fading severity parameter and the average path power is the same for all resolvable paths. In this paper, a detailed performance and tradeoff analysis between the use of the space diversity, path diversity and coding techniques in DS-CDMA system under the Nakagami fading links will be provided.

We will first extend the analysis in [13] to the more general Nakagami fading environment with an arbitrary number of transmitting (Tx) and receiveing (Rx) antennas. The effect of the spatial correlation between receive antenna elements will be addressed. Adopting the moment generating function approach [3], the uncoded BER expression is obtained in the form of a one-fold finite-limit integral, with the integrand being a function of the channel covariance matrix and the operating environment factors.

The exact pairwise error probability is then derived assuming perfect interleaving and soft-decision maximum-likelihood Viterbi decoding. Unlike the common approach using the simple upper bound of the Gaussian Q function, an alternative expression [3] with a finite-limit integral is used. Since the pairwise error probability is exact, our transfer function bound is tighter than that in [23] for the independent fading case, and more general in the framework of MIMO systems. It is worthwhile to note that for dual-MRC diversity using trellis coded modulation in nonselective correlated Nakagami fading channel [24] also uses the similar technique to obtain the exact pairwise error event probability.

The paper is organized as follows. In Section II, we will briefly describe the wideband MIMO channel. Next, the bit error probability of a two-dimensional (2-D) RAKE receiver at the mobile terminal with receive diversity only is presented. In Section IV, the above result is first extended to include dual-transmit diversity using a simple space–time block code [25] and is generalized to the case with an arbitrary number of Tx and Rx antenna elements. The transfer function bound of convolutional-coded BER is derived in Section V. Section VI presents several numerical examples to demonstrate the flexibility of evaluating the impact of individual design parameters on the BER performance of the (2, 2) system. In addition, a tradeoff analysis between the diversity gain and coding gain is presented. Concluding remarks are given in Section VII.

II. Wideband MIMO Channel

We consider the downlink of a W-CDMA system, with M_g antennas at the mobile station (MS) and M_T antennas at the

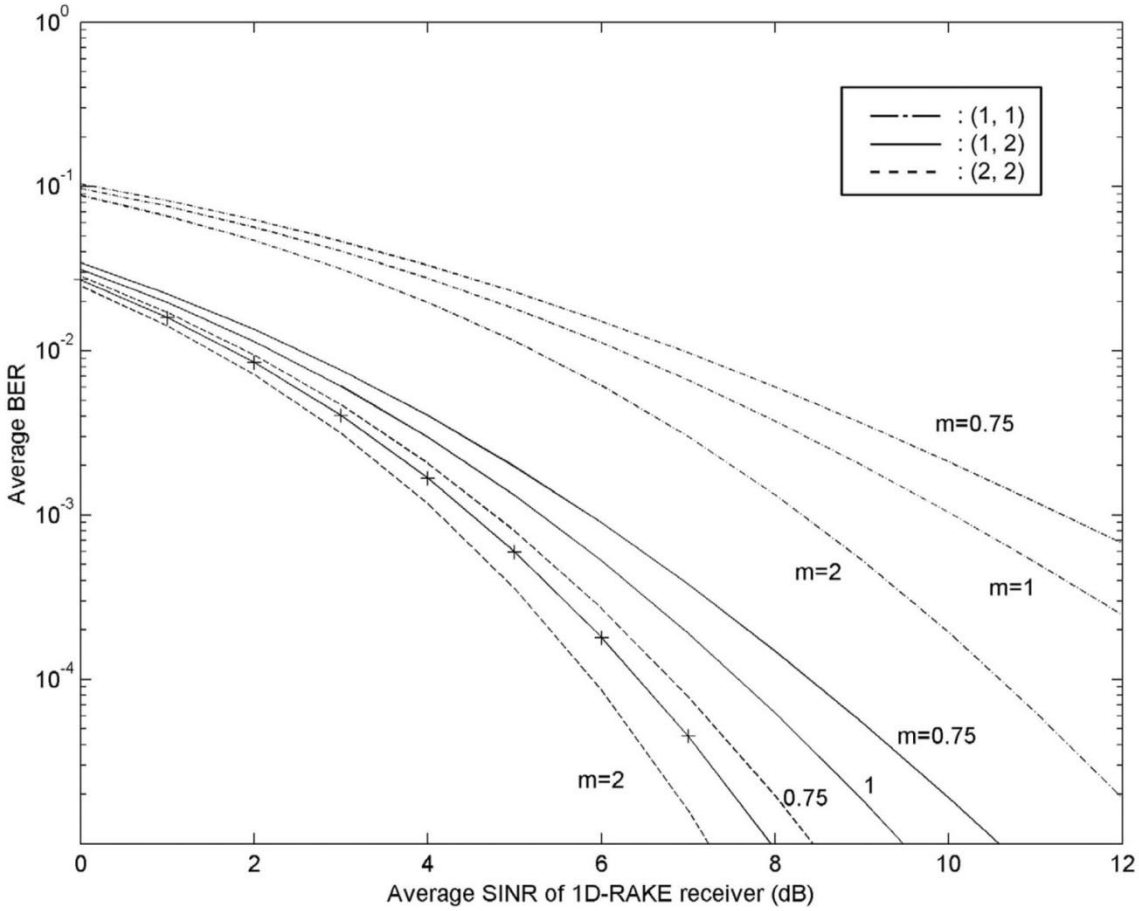

Fig. 2. BER of MAE systems in different Nakagami-m fading channels with constant MIP. For each system, the curves from upper to successively lower position correspond to $\bar{m} = 0.75$, $\bar{m} = 1$, $\bar{m} = 2$. '+' indicates the curve for the (1,2) system in $\bar{m} = 2$ fading overlaps with the (2,2) system in $\bar{m} = 1$ fading channel.

base station (BS). The transmitted and received signals can be represented by

$$\mathbf{s}(t) = [s_1(t)s_2(t)\dots s_{M_T}(t)]^T \tag{1}$$

and

$$\mathbf{r}(t) = [r_1(t)r_2(t)\dots r_{M_R}(t)]^T \tag{2}$$

where ^{T} denotes the vector transpose. The input–output relation of the MIMO system is described by the following vector notation:

$$\mathbf{r}(t) = \mathbf{H} \otimes \mathbf{s}(t) + \mathbf{n}(t) \tag{3}$$

where $\otimes$ denotes the convolution, defined as $c(t) = \int \mathbf{H}^T(\tau)s(t-\tau)d\tau$, and $\mathbf{n}(t)$ includes additive white Gaussian noise and interference.

The general wideband MIMO channel can be modeled as a tapped delay line. Assuming there are L multipath components, the equivalent low-pass vector channel is expressed as

$$\mathbf{H}(\tau) = \sum_{l=0}^{L-1} \delta(\tau - \tau_l)\mathbf{h}^{(l)} \tag{4}$$

where $\delta(\cdot)$ is the Dirac delta function and

$$\mathbf{h}^{(l)} = \left[\, \mathbf{h}_1^{(l)} \quad \mathbf{h}_2^{(l)} \quad \dots \quad \mathbf{h}_{M_T}^{(l)} \,\right] \tag{5}$$

contains M_T SIMO channels $\mathbf{h}_i^{(l)}$, which defines the channel through which the signal is transmitted from Tx antenna i to all Rx antennas at delay τ_l, and each element $h_{ji}^{(l)}$ is the complex channel coefficient from the transmit antenna i at the BS to the receive antenna j at MS. We assume that receive antenna elements experiences identical fading, the paths between each transmit antenna and receive antenna are independent with identical multipath delay profile, and that the fading is constant over at least two consecutive symbol intervals.

In a Nakagami fading channel, the amplitude $\alpha = \left|h_{ji}^{(l)}\right|$ follows Nakagami-m distribution with pdf given in [1] as

$$p(\alpha) = \frac{2}{\Gamma(m_l)} \cdot \left(\frac{m_l}{\Omega_l}\right)^{m_l} \cdot \alpha^{2m_l-1} \cdot e^{-(m_l/\Omega_l)\alpha^2} \tag{6}$$

where $\Gamma(\cdot)$ is the Gamma function, $\Omega_l = \overline{\alpha_l^2}$ is the average power on lth path, and $m_l \geq 1/2$ is the fading parameter, with the special case $m_l = 1$ corresponding to the Rayleigh distribution. Following [7], an exponential multipath intensity profile (MIP) is assumed in the analysis, i.e.,

$$\Omega_l = \Omega_0 e^{-l\delta} \tag{7}$$

where Ω_0 is the average signal strength corresponding to the first incoming path and δ is the rate of average path decay factor, with $\delta = 0$ corresponding to constant MIP assumption as a special case.

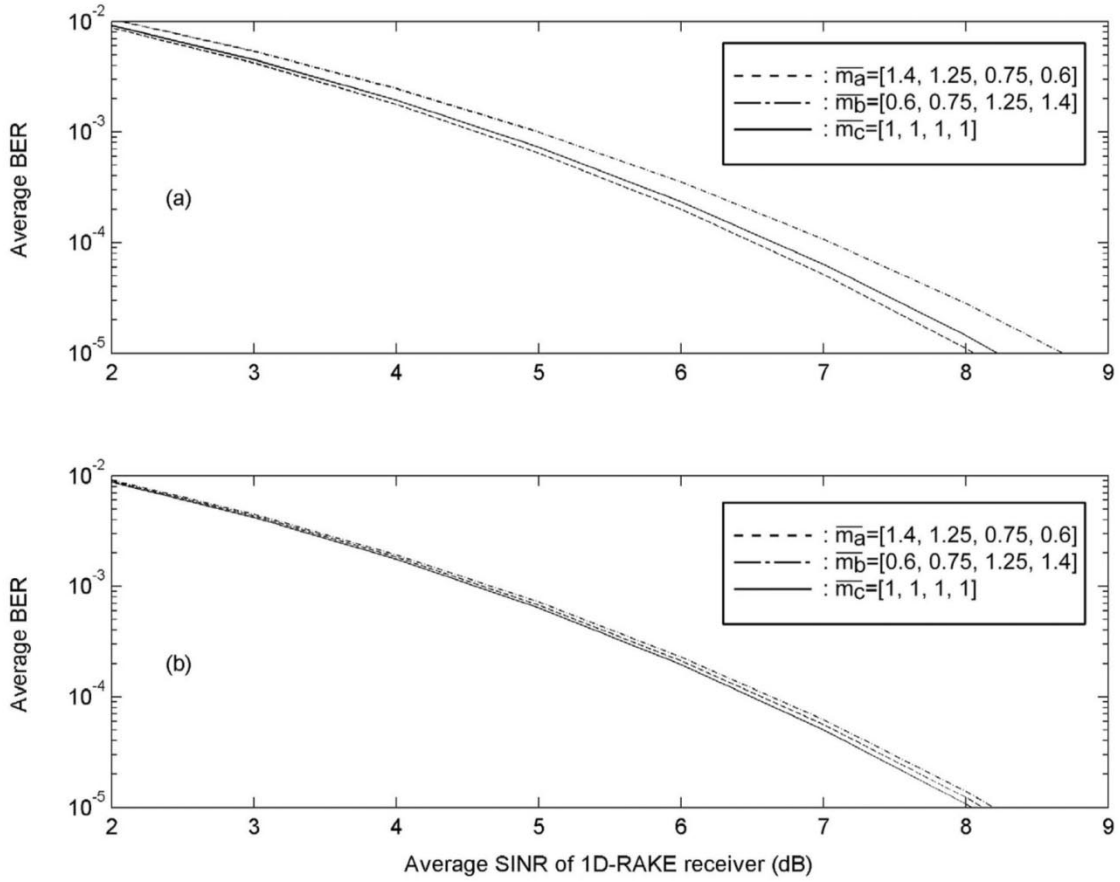

Fig. 3. In a (2, 2) system, comparison between nonidentical fading parameters on different multipaths with identical fading case. (a) $\delta = 0.4$. (b) $\delta = 0.1$.

The potential gain from applying space–time processing is strongly dependent on the spatial correlation coefficient. The most general correlation between the elements of $\mathbf{h}^{(l)}$ may be represented as a four-dimensional (4-D) tensor [9]. Considering that only the immediate surroundings of the antenna array impose the correlation between array elements and have no impact on spatial correlations observed between the elements of the array at the other end of the link [9], we model the correlation among receiver and transmitter array elements independently from one another. It is assumed that BS antennas are sufficiently separated, so that the channels from Tx antenna one or two to Rx antenna array can be assumed to be practically uncorrelated. In the following analysis, we focus on the spatial correlation between receive antennas at MS defined as

$$\rho_{jk}^{(l)} = \left\langle \left|h_{ji}^{(l)}\right|^2, \left|h_{ki}^{(l)}\right|^2 \right\rangle \tag{8}$$

where $\langle a, b\rangle$ represents the correlation between a and b. The formulation in [6] only requires that Gaussian component spatial correlation coefficient $\rho_{jk}^{(l)}$ be given, and the difficulty in looking for the correlation between two Nakagami-faded envelopes is bypassed.

For an M-element uniform linear array (ULA) with omnidirectional elements, the array response vector can be written as

$$\mathbf{v}(\varphi_l) = [\,1 \quad e^{-j2\pi D \sin\varphi_l \lambda} \quad \ldots \quad e^{-j2\pi(M-1)D\sin\varphi_l\lambda}\,]^T \tag{9}$$

where D is the antenna spacing, λ is the carrier wavelength, and φ_l is the mean angle-of-arrival with respect to the axis perpendicular to the line of the array. We refer to $\varphi_l = 0$ as the broadside direction, and $\varphi_l = 90°$ as the end-fire direction.

The closed-form expression of $\rho_{jk}^{(l)}$ for a ULA has been derived assuming that the azimuthual power spectrum (APS) follows a uniform distribution [26], truncated Gaussian distribution [6] and truncated Laplacian distribution [27], respectively, under different propagation conditions. In Section VI, we will use the component spatial correlation derived from a truncated Gaussian APS [6], which is a function of antenna spacing, mean angle-of-arrival (AOA) and the angle spread. It is well known that increasing antenna separation between the antenna elements always reduces their correlation and that the correlation decreases quickly as the angular spread increases.

III. Error Probability Performance of 2-D RAKE Receiver

First, we present the BER performance of a 2-D RAKE receiver without transmit diversity, i.e., $(1, M_R)$ system. Here, we assume perfect channel vector estimation and MRC combining, the instantaneous SINR at the output of 2-D RAKE receiver is given by

$$\gamma = \sum_{l=0}^{L-1} \gamma_l = \sum_{l=0}^{L-1} \sum_{j=1}^{M_R} \gamma_{j,l} \tag{10}$$

where γ_l and $\gamma_{j,l}$ represent the instantaneous signal-to-interference-plus-noise ratio (SINR) on the lth RAKE finger and on the j^{th} antenna array element of the lth RAKE finger, respectively.

For the general case of correlated received signals on antenna elements, the characteristic function of γ_l is given in [6] as

$$\Phi_l(t) = \left| I_{M_R} - it\frac{\bar{\gamma}_l}{m_l} \cdot \mathbf{R}_s^{(l)} \right|^{-m_l} \tag{11}$$

where I_{M_R} is the $M_R \times M_R$ identity matrix, $\mathbf{R}_s^{(l)}$ denotes the $M_R \times M_R$ dimension spatial correlation matrix [6] with each entry being the normalized component correlation coefficient $\rho_{jk}^{(l)}$, and $\bar{\gamma}_l = E_b/N_e \cdot \Omega_l$ is the average SINR per receive antenna contributed from the lth path. Note that E_b is the energy per transmitted bit and N_e is the equivalent power spectral density including AWGN noise and the total interference, which can be approximated as a spatially and temporally white Gaussian noise [7]. Since we assume that all resolvable paths fade independently, the characteristic function of γ is simply

$$\begin{aligned}\Phi(t) &= \prod_{l=0}^{L-1} \left| I_{M_R} - it\frac{\bar{\gamma}_l}{m_l} \cdot \mathbf{R}_s^{(l)} \right|^{-m_l} \\ &= \prod_{l=0}^{L-1} \left| I_{M_R} - it\frac{\bar{\gamma}_0 \cdot e^{-l\delta}}{m_l} \cdot \mathbf{R}_s^{(l)} \right|^{-m_l}\end{aligned} \tag{12}$$

where $\bar{\gamma}_0 = E_b/N_e \cdot \Omega_0$ is the average received SINR corresponding to the first path.

The average bit error probability in the presence of fading is obtained by averaging the conditional error probability over the probability density function (pdf) of γ, i.e., $P_b = \int_0^\infty P(e|\gamma) \cdot p(\gamma) \cdot d\gamma$. The conditional error probability for coherent binary phase-shift keying (CBPSK) is given by [28], i.e., $P(e|\gamma) = Q(\sqrt{2\gamma})$, where $Q(x)$ is the Gaussian Q function. Using the alternative representation of $Q(x)$ given in [3]

$$Q(x) = \frac{1}{\pi}\int_0^{\pi/2} \exp\left(-\frac{x^2}{2\sin^2\vartheta}\right) d\vartheta, \quad x \geq 0 \tag{13}$$

the average BER can then be written as

$$\begin{aligned}P_b =& \frac{1}{\pi}\int_0^\infty \int_0^{\pi/2} \exp\left(-\frac{\gamma}{\sin^2\vartheta}\right) d\vartheta \cdot p(\gamma) d\gamma \\ =& \frac{1}{\pi}\int_0^{\pi/2} \Phi(t)\Big|_{it=-1/\sin^2\vartheta} d\vartheta \\ =& \frac{1}{\pi}\int_0^{\pi/2} \prod_{l=0}^{L-1} \left| I_{M_R} + \frac{\bar{\gamma}_0 \cdot e^{-l\delta}}{m_l \cdot \sin^2\vartheta} \cdot \mathbf{R}_s^{(l)} \right|^{-m_l} d\vartheta.\end{aligned} \tag{14}$$

It is worthwhile to mention that (14) applies to very general channel conditions, specifically: 1) the path signal arriving at different antenna elements can be arbitrarily correlated, but experiences the same fading severity; 2) different resolved multipath signals that are faded independently, can have the fading statistics coming from different Nakagami families, i.e., the fading parameters are not necessarily equal for all RAKE fingers; 3) the average SINRs may be nonidentical for different paths, assuming exponential path delay profile to characterize the average power at the output of the channel as a function of the path delay.

By setting $M_R = 2$, the average BER for the dual diversity receiver is obtained as (15), shown at the bottom of the page.

For $M_R > 2$, the integrand of (14) expressed in terms of spatial correlation becomes cumbersome, the alternative representation of the determinant of the matrix is desirable. Since $\mathbf{R}_s^{(l)}$ is positive definite, it can be easily shown, through eigen-decomposition, that the following equation holds for any real, positive g:

$$\left| I_{M_R} + g \cdot \mathbf{R}_s^{(l)} \right| = \prod_{i=1}^{M_R} (1 + g \cdot \lambda_{l,i}) \tag{16}$$

where $\{\lambda_{l,i}\}_{i=1}^{M_R}$ are the eigenvalues of $\mathbf{R}_s^{(l)}$. Therefore, (14) can be rewritten as

$$P_b = \frac{1}{\pi}\int_0^{\pi/2} \prod_{l=0}^{L-1} \prod_{i=1}^{M_R} \left(1 + \frac{\bar{\gamma}_o \cdot e^{-l\delta}}{m_l \cdot \sin^2\vartheta} \cdot \lambda_{l,i}\right)^{-m_l} d\vartheta. \tag{17}$$

For independent antenna branches, i.e., $\lambda_{l,i} = 1$, $l = 0, \ldots, L-1$, $i = 1, \ldots, M_R$, (17) is simplified to

$$P_{b,indep} = \frac{1}{\pi}\int_0^{\pi/2} \prod_{l=0}^{L-1} \left(1 + \frac{\bar{\gamma}_o \cdot e^{-l\delta}}{m_l \cdot \sin^2\vartheta}\right)^{-M_R \cdot m_l} d\vartheta. \tag{18}$$

Furthermore, under the assumptions that all multipaths experience the same extent of fading and constant MIP, we have

$$P_b = \frac{1}{\pi}\int_0^{\pi/2} \left(1 + \frac{\bar{\gamma}_o}{m \cdot \sin^2\vartheta}\right)^{-M_R \cdot L \cdot m} d\vartheta. \tag{19}$$

This is equivalent to the performance with $M_R \cdot L$ independent diversity branches in Nakagami fading. Substituting $M_R = 1$ in (19) leads to the same expression as [4].

IV. Error Probability of MIMO Systems

For the purpose of illustration, the simple dual transmit diversity space–time block code proposed by Alamouti [25] is adopted in the analysis. The QPSK symbols d_1 and d_2 are transmitted simultaneously from antenna 1 and antenna 2, respectively. In the next symbol interval, the symbol $-d_2^*$ is transmitted

$$P_b = \frac{1}{\pi}\int_0^{\pi/2} \prod_{l=0}^{L-1} \left[\left(1 + \frac{\bar{\gamma}_o \cdot e^{-l\delta}}{m_l \cdot \sin^2\vartheta}\right)^2 - \left(\frac{\bar{\gamma}_o \cdot e^{-l\delta}}{m_l \cdot \sin^2\vartheta}\right)^2 \cdot \left|B_{12}^{(l)}\right|^2\right]^{-m_l} d\vartheta. \tag{15}$$

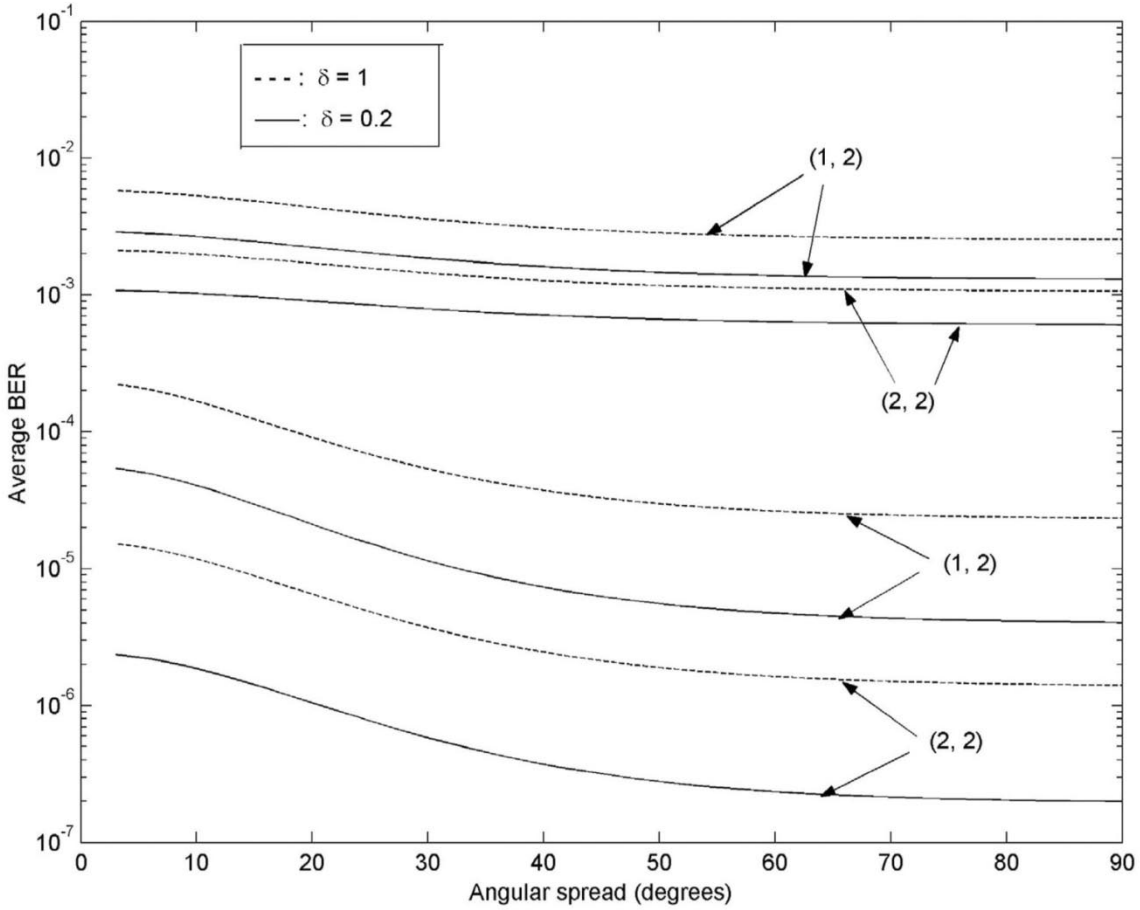

Fig. 4. Angular spread's effect on BER performance of (1, 2), (2, 2) systems, in $\bar{m} = 1.2$ fading channel, the upper group is at $\bar{\gamma} = 5$ dB, and the lower group is at $\bar{\gamma} = 10$ dB.

from antenna 1 and the symbol d_1^* from antenna 2. Alamouti [25] has shown that the maximum likelihood (ML) estimates of the transmitted data are identical to the ML estimates obtained in a system with a single-transmit antenna and dual-receive antennas. Therefore, the SINR at the output of 1-D RAKE receiver can be expressed as

$$\gamma = \frac{1}{2}\sum_{l=0}^{L-1}(\gamma_{1,l} + \gamma_{2,l}) \tag{20}$$

where the factor $\frac{1}{2}$ is due to sharing of the transmitted signal power between two antennas.

Combining both transmit and receive diversity

$$\gamma = \frac{1}{2}\sum_{l=0}^{L-1}\sum_{j=1}^{M_R}(\gamma_{j1,l} + \gamma_{j2,l}) \tag{21}$$

where $\gamma_{j1,l}$ and $\gamma_{j2,l}$ are the SINRs of the lth path signal from the first and second Tx antenna to the jth receive antenna, respectively. Since the channels from different transmit antennas to the receiver array are assumed to be independent and identically distributed, the characteristic functions of $\gamma_{j1,l}$ and $\gamma_{j2,l}$ have the same form as (11), with the average path SINR equal to $\overline{\gamma}_l/2$. Finally, we have

$$\Phi_\gamma(t) = \prod_{l=0}^{L-1}\left|I_{M_R} - it\frac{\bar{\gamma}_l}{2m_l}\cdot\mathbf{R}_s^{(l)}\right|^{-2m_l}. \tag{22}$$

The BER is given by

$$\begin{aligned} P_b =& \frac{1}{\pi}\int_0^{\pi/2}\Phi_\gamma(t)\Big|_{it=-1/\sin^2\vartheta}d\vartheta \\ =& \frac{1}{\pi}\int_0^{\pi/2}\prod_{l=0}^{L-1}\left|I_{M_R} + \frac{\bar{\gamma}_0\cdot e^{-l\delta}}{2m_l\cdot\sin^2\vartheta}\cdot\mathbf{R}_s^{(l)}\right|^{-2m_l}d\vartheta. \end{aligned} \tag{23}$$

It is straightforward to show that the BER of a general (M_T, M_R) MIMO system can be extended from (23) as follows:

$$P_b = \frac{1}{\pi}\int_0^{\pi/2}\prod_{l=0}^{L-1}\left|I_{M_R} + \frac{\bar{\gamma}_0\cdot e^{-l\delta}}{M_T\cdot m_l\cdot\sin^2\vartheta}\cdot\mathbf{R}_s^{(l)}\right|^{-M_T\cdot m_l}d\vartheta. \tag{24}$$

It is necessary to point out that the derivation of (23) is based on the use of space–time block codes from orthogonal designs.

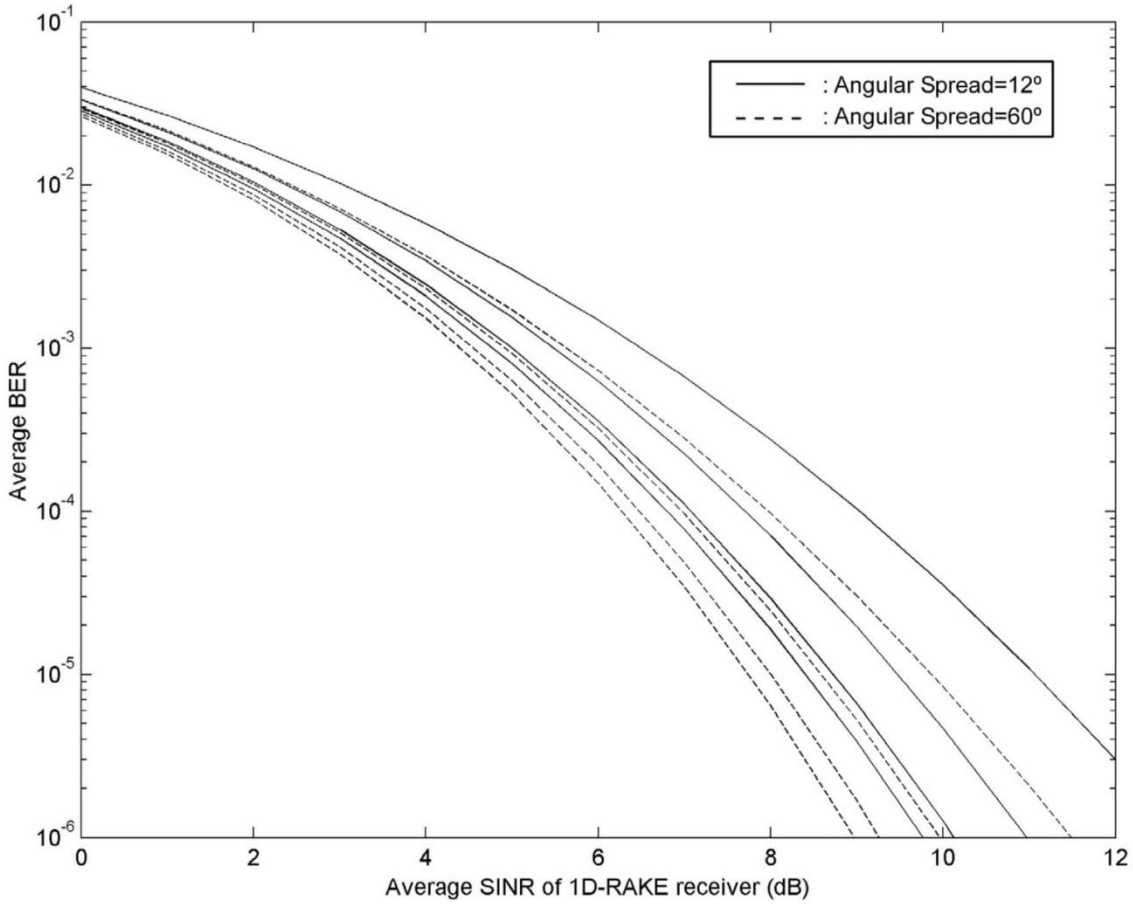

Fig. 5. BER of a (2, 2) system in $\bar{m} = 1.2$ fading channel, with different MIP decay factor. The solid lines depict $\delta = 2, 1, 0.5, 0$ in successively lower position for small angular spread case, and the dashed curves are for large angular spread case.

TABLE I
MAXIMUM FREE DISTANCE CONVOLUTIONAL CODES

n	k	C_L	d_{free}	Generators (in octal)
2	1	7	10	133, 171
2	1	4	6	15, 17
3	1	4	10	13, 15, 17
4	1	3	10	5, 7, 7, 7
4	1	4	13	13, 15, 15, 17

However, [30] proved that for complex orthogonal designs, only $M_T = 2$ Alamouti-code can provide the maximum possible transmission rate and full diversity. For $M_T > 2$, the space–time block codes can give full diversity, but lose up to half of the theoretical bandwidth efficiency. Therefore, the generation from (23) to (24) is only valid for real constellations or with the loss in bandwidth for complex constellation.

V. COMBINED CODING AND DIVERSITY

In mobile radio communication systems, FEC techniques are employed to protect the information against the severe fading due to multipath propagation. Moreover, it is well known that in spread spectrum systems, the use of channel coding does not require additional allocation of bandwidth [15]. On a fading channel, coding should be used with techniques which decorrelate the received energy of each consecutive coded symbol. Interleaving is one of these techniques and used to "break up" the memory in the fading process due to Doppler spread, and make burst errors into random errors, which can be efficiently corrected by an error correcting code. The length of the interleaver can be adjusted to match the fading characteristics of the channel.

For a fading channel, the appropriate performance measure of a convolutional coded system is the average BER P_e at the output of the Viterbi decoder. The convolutional code will be denoted by $(n\,, k\,, C_L\,)$, where n is the number of encoded output bits per k binary input information bits, and C_L is the code constraint length. Following the usual transfer function bound [28] for ML decoding over memoryless channels, the average bit error probability of a rate $r_c = k/n$ linear convolutional code may be bounded as

$$P_e \leq \frac{1}{k} \sum_{d=d_{\text{free}}}^{\infty} \beta_d P_2(d) \tag{25}$$

where d_{free} is the free distance of the code, the $\{\beta_d\}$ are the coefficients in the expansion of the derivative of $T(D, N)$, the transfer function of the code, evaluated at $N = 1$ [29], and $P_2(d)$ is the average pairwise error probability of selecting an incorrect path $\underline{x}'$ in the trellis that merges with the all-zero path

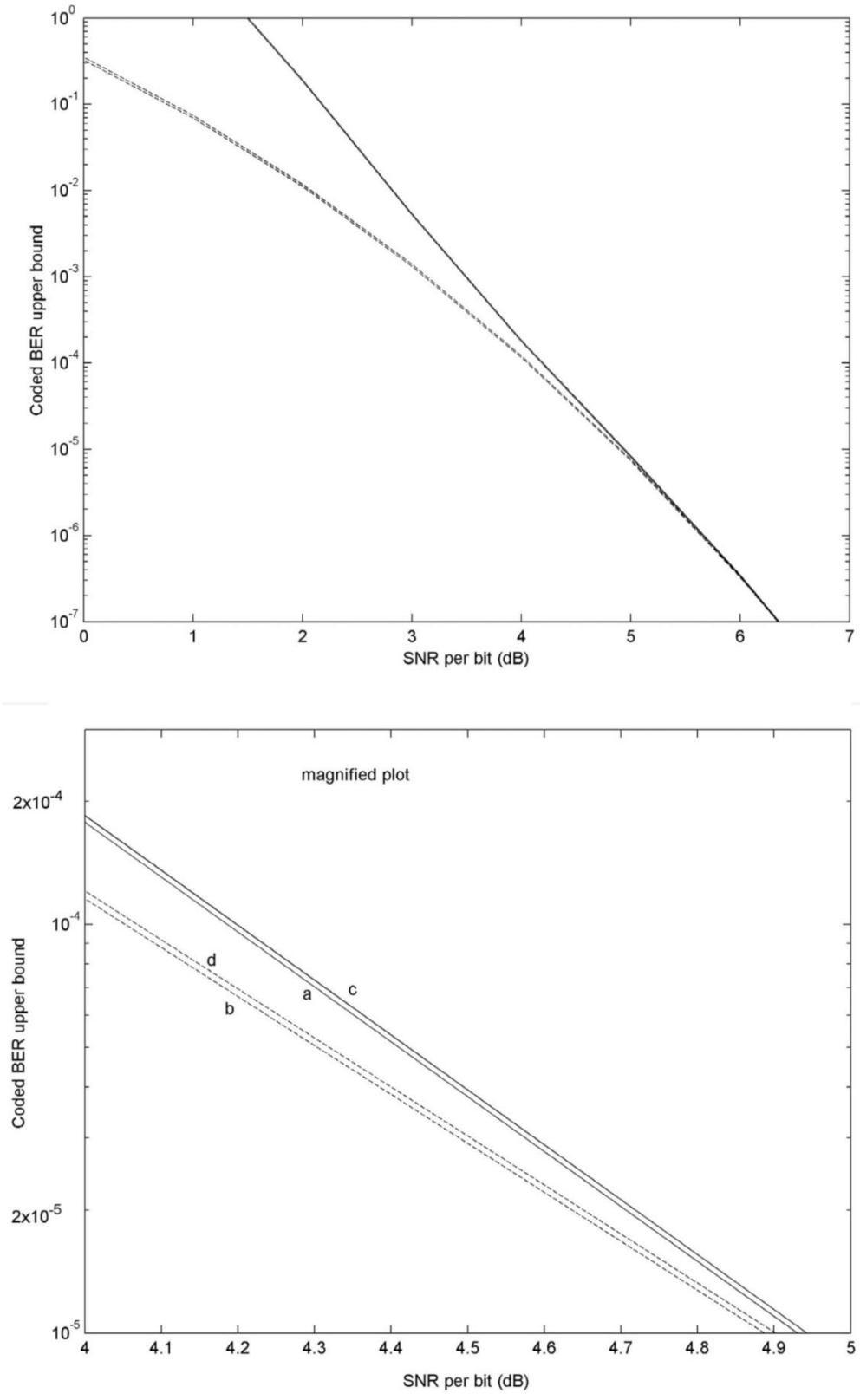

Fig. 6. Comparison of bounds using (29) and the exact pairwise error probability (28) in the two-path $\bar{m} = 2$ fading channel.

$\underline{x}$ for the first time, and $\underline{x}'$ differs from $\underline{x}$ in d bit positions. When using the transfer function bound, the channel characteristics affect only the pairwise error probability between codewords. The derivation of $P_2(d)$ is the emphasis of this section.

An error is made if the squared Euclidean distance metric of $\underline{x}'$ is less than that of $\underline{x}$, or equivalently, if the difference of metrics is negative. For binary modulation techniques, the squared Euclidean distance between a pair of paths is proportional to

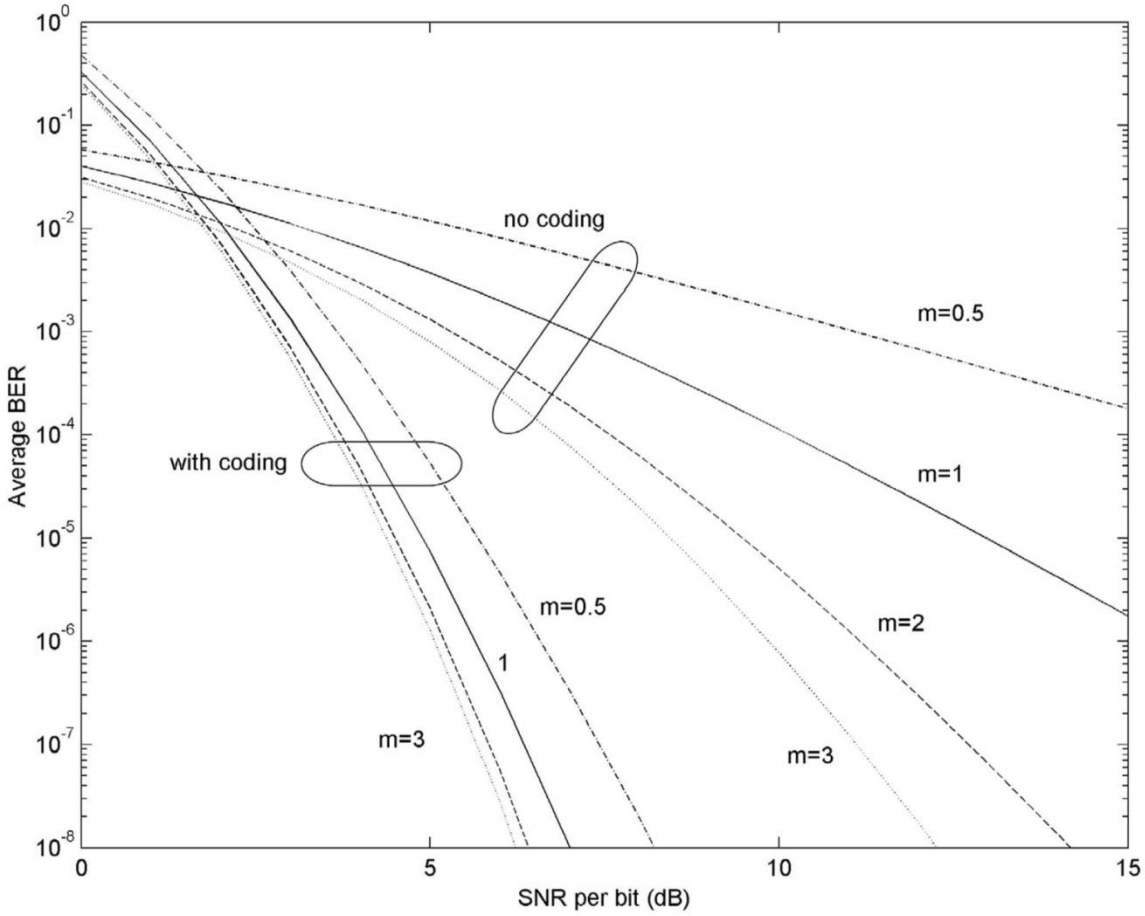

Fig. 7. Uncoded and coded BER of a (2, 2) system in different Nakagami fading channels with two resolvable paths.

the sum of the received energy of their differing code symbols (for other nonbinary techniques, the results presented here have to be modified by using a weighted sum of received energy.) Let the path $\underline{x}'$ and $\underline{x}$ differ in d bit positions $i_1, i_2, \ldots i_d$, then the energy sum of the different codesymbols may be written as $\varepsilon(\underline{x}', \underline{x}) = \sum_{n=1}^{d} \varepsilon(i_n)$, where $\varepsilon(i_n)$ denotes the energy of i_n th bit.

Assuming MRC and unquantized demodulator outputs, the conditional pairwise error probability for BPSK modulated signals is simply $Q\left(\sqrt{2\varepsilon(\underline{x}', \underline{x}/N_e}\right)$. For a (1, M_R) system in an L-path selective fading channel, we have

$$P_2(d) = E\left[Q\left(\sqrt{\frac{2E_s}{N_e}\sum_{n=1}^{d}\sum_{l=0}^{L-1}\sum_{j=0}^{M_R-1}\left|h_j^{(l)}(i_n)\right|^2}\right)\right] \equiv E\left[Q\left(\sqrt{\frac{2E_s}{N_e}\sum_{n=1}^{d}\hbar_n^2}\right)\right] \tag{26}$$

where $h_j^{(l)}$ is defined as the channel coefficient to j^{th} receive antenna for lth path, $\hbar_n^2 \equiv \sum_{l=0}^{L-1}\sum_{j=0}^{M_R-1}\left|h_j^{(l)}(i_n)\right|^2$, $E[\cdot]$ denotes the expectation, and the expectation is taken with respect to the channel states $\hbar_n$. Since we assumed that ideal interleaving and deinterleaving make the $\hbar_n$s i.i.d. random variables, the average over $\{\hbar_n\}$ can be computed as the product of averages. Consequently, the characteristic function of the overall SINR can be represented by the product of the characteristic function of each code symbol's SINR. Following the similar derivation in Section III, the average pairwise error probability for a (M_T, M_R) system can be written as

$$P_2(d) = \frac{1}{\pi} \times \int_0^{\pi/2}\prod_{l=0}^{L-1}\left|I_{M_R} + \frac{\bar{\gamma}_0 \cdot e^{-l\delta}}{M_T \cdot m_l \cdot \sin^2\vartheta} \cdot \mathbf{R}_s^{(l)}\right|^{-M_T \cdot m_l \cdot d} d\vartheta. \tag{27}$$

In the numerical examples, we will compare the bound using (27) with that derived in [23], i.e.,

$$P_2(d) < \frac{\Gamma(dm_T - \frac{1}{2})}{2\sqrt{\pi}\cdot\Gamma(dm_T)} \times \sqrt{\frac{\frac{r_c E_b \Omega_T}{N_0} + m_T}{\frac{r_c E_b \Omega_T}{N_0}}}\left(\frac{r_c E_b \Omega_T}{m_T N_0} + 1\right)^{-dm_T} \tag{28}$$

where $m_T = \sum_{l=0}^{L-1} m_l$, $\Omega_T = \sum_{l=0}^{L-1} \Omega_l$.

It is worthwhile to note that here again, we use the alternative expression of Q-function (13), as oppose to using its simple upper bound [23]. Thus, the pairwise error probability (27) is exact, which makes our bound always tighter than that using (28), since (27) is the sum over all possible error events of the **exact** values of the pairwise probability of those events.

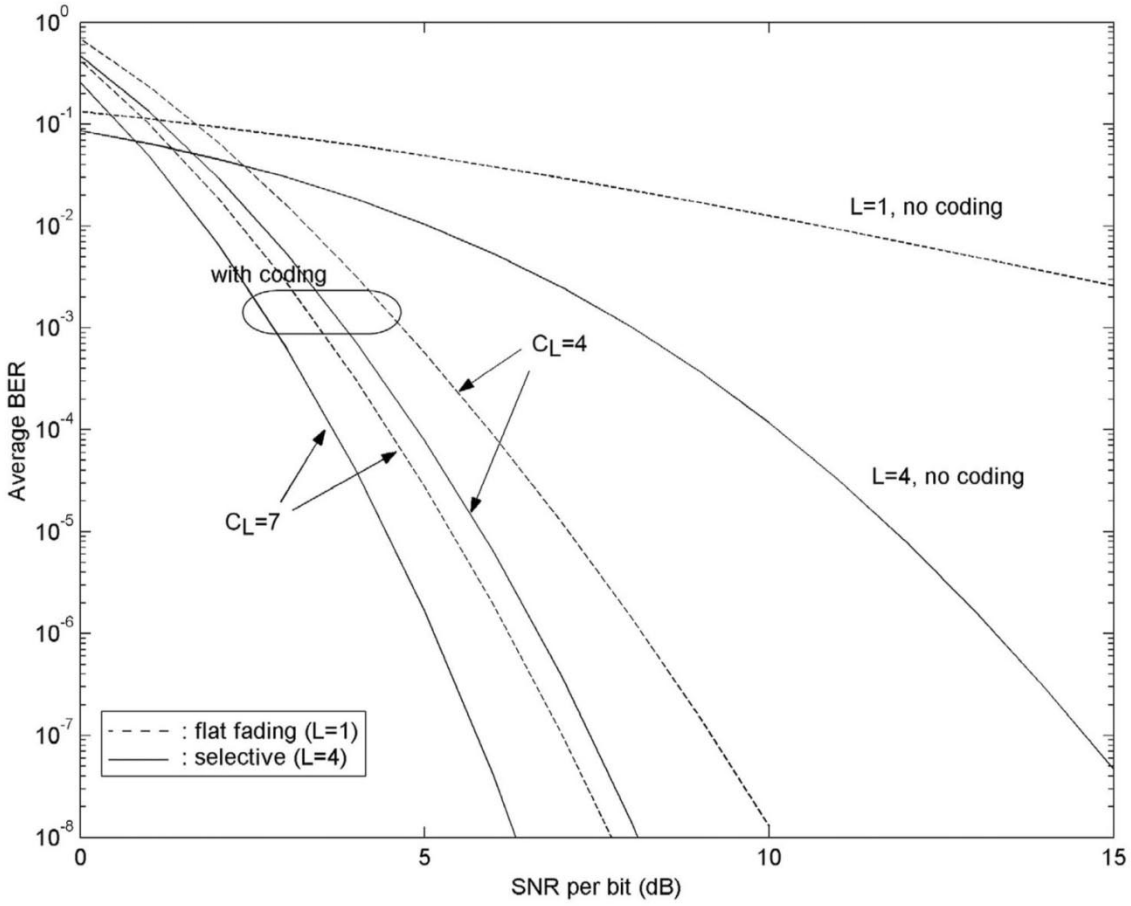

Fig. 8. Performance in flat fading (dash curves) or selective fading (solid curves) channel with two Rx antennas separated by $\frac{1}{4}$ wavelength, angular spread $\sigma = 60°$, and two codes with the same coding rate 1/2 and different constraint lengths.

VI. Numerical Examples

In this section, we present selected numerical results to illustrate the impacts of the operating environment (i.e., the angular spread, the path decay factor and fading parameters) on the BER performance of the (2, 2) MAE system in correlated Nakagami-m fading channels, and to illustrate the benefits of combined coding and diversity techniques. For notational simplicity, the Nakagami fading parameters used in each plot is given as a vector $\bar{m} = [m_0, m_1 \ldots m_{L-1}]$ of length L, corresponding to the L resolvable paths at the receiver. In the case that the fading parameters are identical along all the resolvable paths, we simply give that value, e.g., $\bar{m} = 0.75$ implies that all paths undergo identical Nakagami fading with the fading parameter 0.75. It is assumed that the total transmit power is fixed, regardless of the number of transmit antenna elements, and uniform power is allocated to each transmit antenna. The total received power from all paths is also assumed to be the same for various power decay factors δ of the exponential decaying MIP. In the first five examples, $L = 4$ resolvable paths, broadside reception, and antenna separation $D = 1/2\lambda$ are assumed, unless otherwise specified. The no transmit or receive diversity case (1, 1) is plotted to calculate the overall spatial-path diversity gain.

Fig. 1 plots the average BER of various MAE systems in Rayleigh fading with the constant MIP, as a function of the average received SINR of 1-D RAKE receiver, i.e., $E_b \cdot \sum_{l=0}^{L-1} \Omega_l / N_e$. We can clearly see the performance with transmit only diversity, i.e., (2, 1) and (4, 1) systems are 3 and 6 dB worse than the receive-only diversity, (1, 2) and (1, 4) systems, respectively. This is because each transmit antenna radiates half or one-quarter of the energy in order to ensure the same total radiated power as with only one transmit antenna. If each transmit antenna was to radiate the same energy, the performance of (M_T, M_R) and (M_R, M_T) would be identical. At BER $= 10^{-4}$, the diversity gains for (2, 1), (1, 2) and (2, 2) systems are 2.5, 5.5, and 6.8 dB, respectively. It is necessary to point out that the overall diversity gain comes from two sources: 1) reducing the range of fading fluctuation through intelligent combining of several dissimilarly fading signals and 2) the additional average power since the average power extracted from the received field is proportional to the number of receive antennas. Another important observation is that for the systems having the identical value of $M_T \times M_R$, the average BER curves are asymptotically parallel to each other. This is because for large SINR, the average BER varies asymptotically as the inverse $(M_T \times m \times M_R \times L)^{\text{th}}$ power of SINR, which provides the effective order of diversity equal to $(M_T \times m \times M_R \times L)$.

In Fig. 2, the effect of fading parameter on BER are shown for (1, 1), (1, 2), and (2, 2) systems, assuming independent receive signals and the constant MIP. Large fading parameter means less severe fading occurs, as indicated by the improvement in BER.

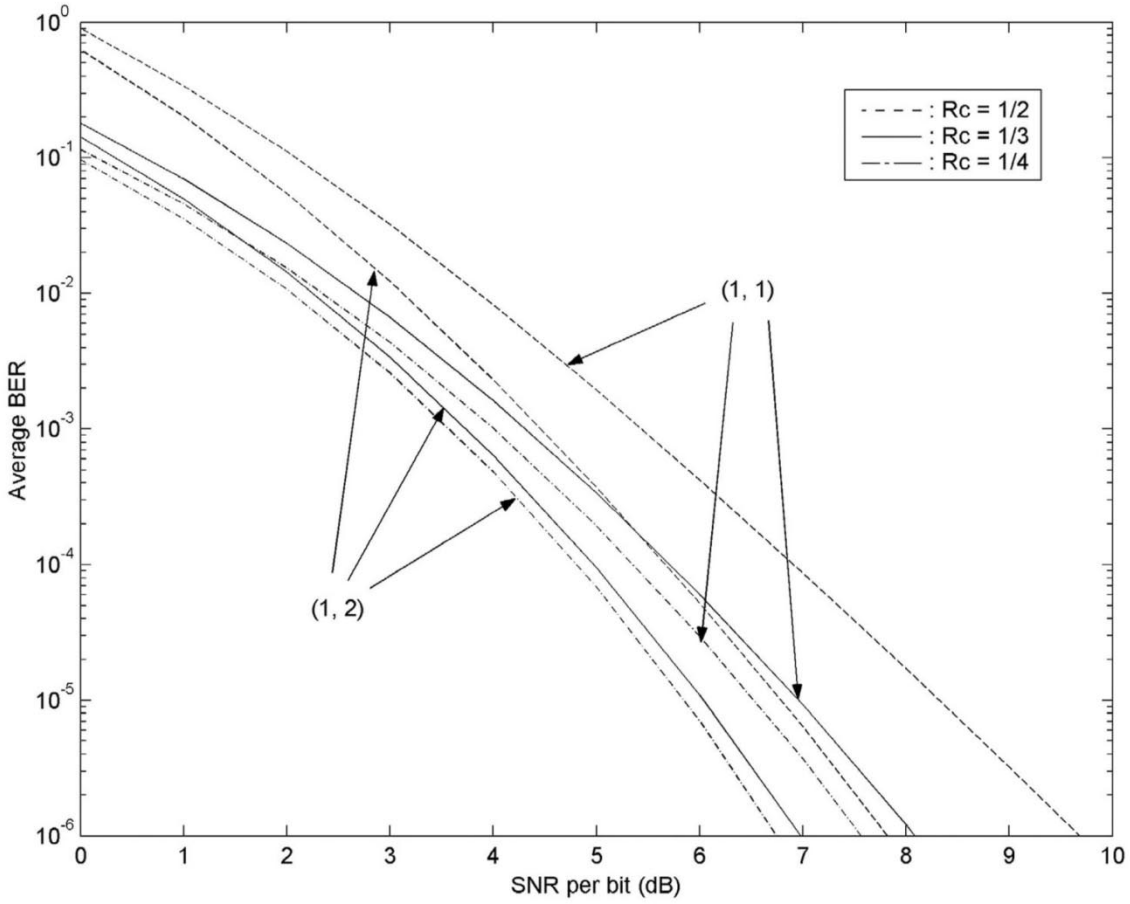

Fig. 9. Performance comparison employing three convolutional codes with the same constraint length and different coding rates: (2,1,4), (3,1,4), and (4,1,4).

We note that the curve of (1, 2) in $\bar{m} = 2$ fading overlaps with that of (2, 2) in $\bar{m} = 1$ fading. This is not a surprising result, as (24) shows. This means that under the total transmitted power constraint, adopting M_T fold transmit diversity is equivalent to operating the same receiver in the $M_T \cdot \overline{m}$ fading channel.

Fig. 3 shows the difference when arbitrary fading parameters for the different paths are compared to the identical case. For illustration, we choose the arbitrary multipath fading parameter vector to be $\bar{m}_a = [1.4, 1.25, 0.75, 0.6]$, $\bar{m}_b = [0.6, 0.75, 1.25, 1.4]$. This selection has the same mean value as $\bar{m}_c = 1$. It is obvious that performance differences exist, and the amount of difference increases for higher value of power decay factor. When the channel has rapid path decay, e.g., $\delta = 0.4$, if the paths with higher average power (corresponding to paths with small path delays) suffer more severe fading (e.g., in $\bar{m}_b$ channel), the diversity gain is less than the one obtained with identical fading parameter, and the diversity gain in $\bar{m}_a$ channel is larger than that in identical fading channel. In the channel with small δ or with constant MIP, identical fading along all the resolved paths gives the best performance.

The impact of the angular spread is illustrated in Fig. 4 at two fixed SINR levels, $\bar{\gamma} = 10$ dB and $\bar{\gamma} = 5$ dB, with antenna spacing $D = 1/4\lambda$, in $\bar{m} = 1.2$ fading channel. Large angular spread increases the spatial selectivity of the channel, thereby increasing the space diversity gain. At the low average SNR level, the performance variation with change of angular spread is small. For example, at $\bar{\gamma} = 5$ dB, the BER for $\sigma = 3°$ is only twice as high as that of $\sigma = 90°$, while at $\bar{\gamma} = 10$ dB, the BER of $\sigma = 3°$ is about 10 times as high as that of . The sensitivity to angular spread seems independent of the power decay factor, and comparable in (2, 2) and (1, 2) systems.

Fig. 5 compares the performance of a (2, 2) system in the channel with various power decay factors in $\bar{m} = 1.2$ fading channel. The dash lines depict the larger angular spread signals ($\sigma = 60°$) with $\delta = 2$,1, 0.5, 0 in successively lower positions. The solid curves show the corresponding δ for the $\sigma = 12°$ case. δ reflects the frequency selectivity of the channel and, thus, as δ decreases, the gain due to path diversity is increased. In the case of large δ, like in an indoor environment, the angular spread can be large, which provides efficient space diversity. In the contrary case, when both δ and σ are small, the path diversity will be efficient. This result indicates the synergy of space and path diversity. The effects of σ, δ and fading parameters on BER performance indicate that the performance of MAE system depends strongly on the operational environment.

In the above examples, we focused on 2-D RAKE receiver's space-path diversity without coding. In the following, we will determine the effects of different code rates and constraint lengths on the coded DS-CDMA system, as well as the tradeoff between the diversity gain and the coding gain. Table I lists the parameters of several low rate maximum free distance codes

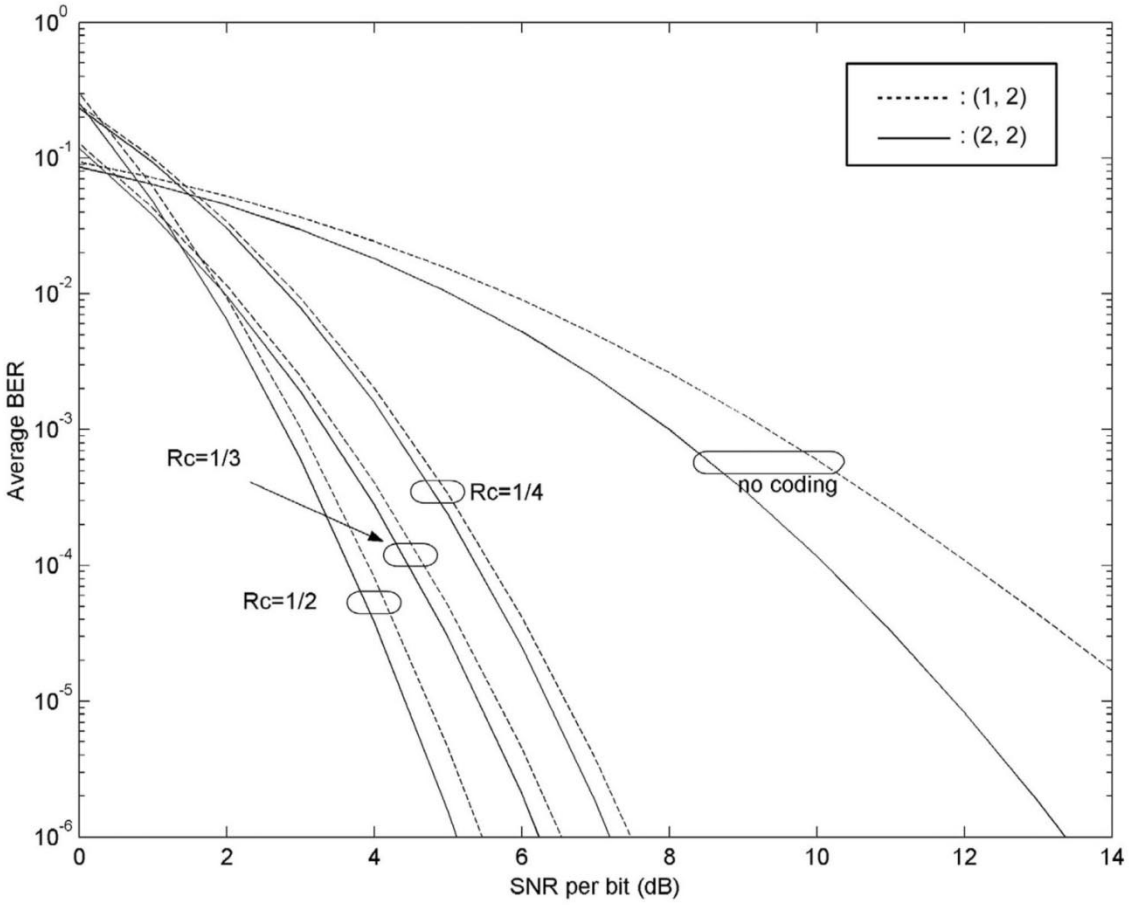

Fig. 10. Performance comparison employing three convolutional codes with the same free distance and different coding rates: (2,1,7), (3,1,4) and (4,1,3).

[29], which will be used in the numerical evaluation. For a fair comparison between the coded and uncoded system, the total energy used for transmitting k information bits is assumed to be equal to that used for transmitting n coded bits. That is to say, E_b is the energy per information bit.

First, we will compare the performance bounds obtained by substituting (27) and (28)[23] into (25), using a (2, 1, 7) convolutional code in $\bar{m} = 2$ fading channel. This code has the free distance $d_{\text{free}} = 10$ and only even Hamming weight [29] paths. Identical fading parameters along all paths and constant MIP in a (1, 1) system are chosen to meet the condition of using (28). In Fig. 6, curves a and b are computed by substituting (27) into (25), and curves c and d correspond to substituting the pairwise error probability bound (28) in (25). Specifically, curves a and c are obtained by summing over the first 18 terms of the series expansion of the bound in (25), while curves b and d only use the first six terms. The magnified SNR range is shown below. It can be seen that our bound (27) is consistently tighter than (28) over the entire SNR range, although the difference is negligible for $SNR > 2$ dB. The diverging behavior at low SNR is typical for transfer function type union bounds [23]. Note that the curve computed by using the first six terms of the series expansion of the bounds in (25) very accurately approximates the simulation result as demonstrated in [23], we will only sum the pairwise error probabilities for the six shortest Hamming distances as the coded BER upper bound in the following examples.

In order to emphasize the space diversity gain due to combining only, BER will be plotted versus SNR per bit, defined as the average SINR per information bit per antenna, under the constraint that the total received SINR is fixed regardless of the value of M_R. To further narrow our focus, constant MIP and identical path fading parameters are employed in the following examples.

Fig. 7 shows the uncoded BER and coded BER (using a (2, 1, 7) code) upper bound of a (2,2) system in different Nakagami fading channels with two resolvable paths. The performance improvement achieved by coding is shown to be very impressive. Since the free distance $d_{\text{free}} = 10$ results in a coding gain which has the similar effect as introducing tenth-order diversity, the coded system has an order of diversity equal to $(M_T \times m \times M_R \times L \times d_{\text{free}})$. In addition, the coded system exhibits a smaller performance difference in varying fading channels compared with uncoded system. This results in more significant coding gain in severe fading channels.

Next in Fig. 8, we consider two Rx antennas separated by $\frac{1}{4}$ wavelength, with an angular spread of $\sigma = 60°$, (which gives a spatial correlation of approximately 0.53,) operating in the flat fading or frequency selective fading channel with $\bar{m} = 0.75$. The comparison between applying the (2,1,7) and the (2,1,4) codes indicates that by increasing the convolutional code constraint length, the performance becomes better due to the larger free distance. However, the decoding complexity increases ex-

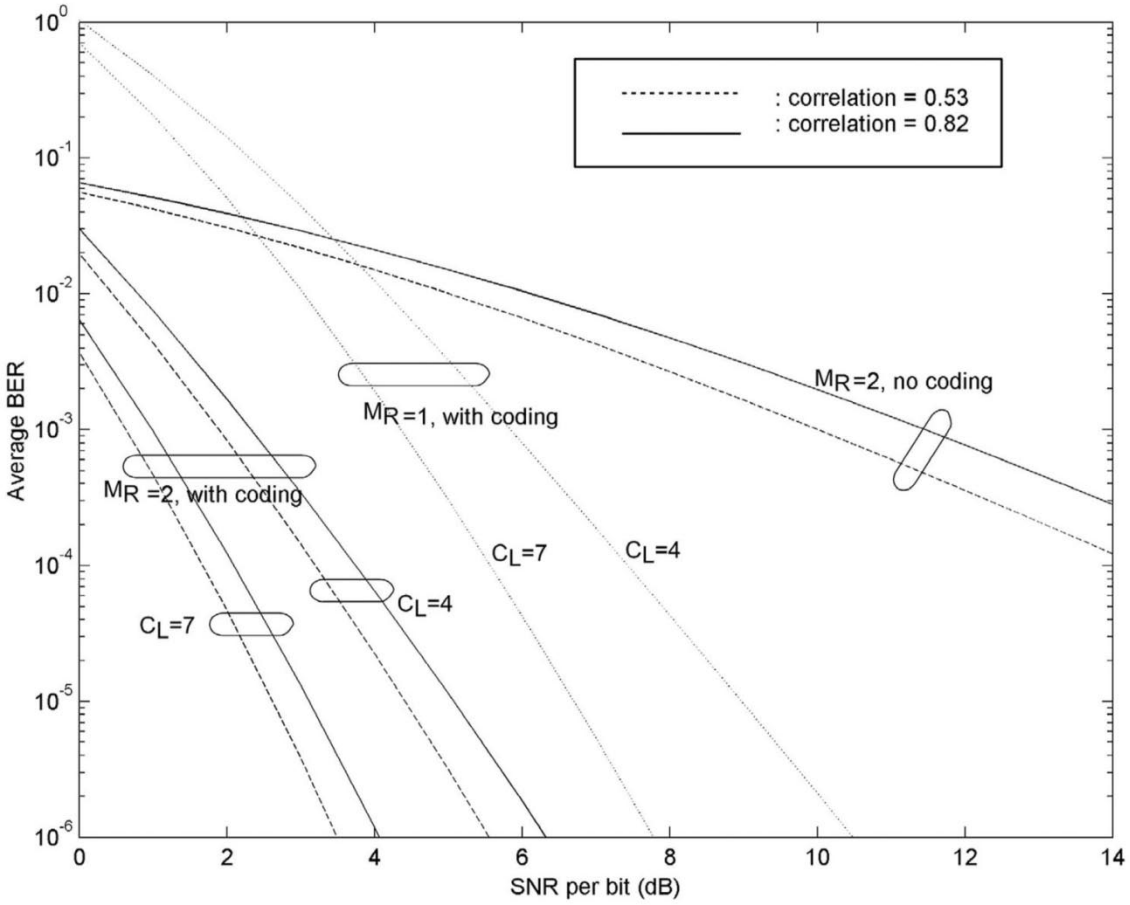

Fig. 11. Performance comparison of different coding and diversity schemes in $\bar{m} = 1.25$ fading channel.

ponentially with C_L. The achievable coding gain is smaller in the case of $L = 4$ multipath components compared with signalling over the frequency nonselective channel ($L = 1$).

Three codes with the same constraint length $C_L = 4$ and different coding rates applied in (1,1) and (1,2) systems are compared in Fig. 9. Independent antenna branches in a two-path, $\bar{m} = 0.75$ fading channel are assumed. It is not surprising that for a fixed number of Rx antennas, the performance is improved with decreasing code rate. On the other hand, the more powerful the code, the smaller the gain realized by space-path diversity. For example, at $BER = 10^{-5}$, dual Rx antennas provide 1.4 and 0.7 dB diversity gain when applying $r_c = 1/2$, 1/4 codes, respectively. This fact leads to the conclusion that with powerful codes, the main purpose of the 2-D RAKE receiver is to collect the power distributed in various propagation paths, not to improve the performance by introducing additional diversity.

Next, we compare three codes with the same $d_{\text{free}} = 10$ in a two-path $\bar{m} = 1.25$ fading channel. Since with soft-decision decoding, the upper bound on the coded BER drops by d_{free} orders of magnitude as the SNR is increased over a range of 10 dB, the average BER of these three codes exhibits the same asymptotic slope, as indicated in Fig. 10. On the other hand, there is approximately 1 dB difference between using the codes (2,1,7) and (3,1,4), and also between the codes (3,1,4) and (4,1,3). It can be concluded that with the identical free distance, the code with higher coding rate gives better performance, resulting from larger $r_c \cdot \overline{\gamma}_0$ in the evaluation of the pairwise error probability (27).

Finally, Fig. 11 illustrates the BER performance of different coding and diversity schemes versus the average received SINR of a 1-D RAKE receiver. Specifically, we consider the single Tx and Rx antenna system employing codes (2,1,7) and (2,1,4), and (1, 2) system with or without coding, in a single-path $\bar{m} = 1.25$ fading channel. To illustrate the tradeoff between space-path diversity gain and coding gain, we allow the total received power to be proportional to the number of receive antennas. For dual-Rx antennas, two angular spreads $\sigma = 60°$ and $\sigma = 25°$ are assumed, giving spatial correlations equal to 0.53 and 0.82, respectively. It is observed that the performance with antenna diversity alone is better than the coded system with a single antenna up to a certain SNR threshold, and above which the performance is degraded relative to the coded single antenna case. The threshold depends on various factors, such as fading severity, the coding scheme, the spatial correlation and the number of Tx and Rx antennas. Thus, adding diversity, especially at a low SNR level, can effectively reduce the number of bit errors at the convolutional decoder input, thus the advantages of coding can be fully exploited.

VII. Conclusion

We derived the BER of a general MIMO system using maximal ratio combining and open loop transmit diversity in corre-

lated Nakagami fading channels. The closed-form analytical expression was given in the simple form of a single finite limit interval, with the integrand being an elementary function of array configuration parameters, spatial correlation, and operating environment factors, including angular spread, path decay factor, and fading parameters. Furthermore, we incorporated the exact pairwise error probability into the transfer function bound, so that the well-known performance advantages of convolutional codes in Rayleigh fading are extended to the general MIMO system in frequency selective Nakagami fading. The overall diversity (asymptotic slope) is equal to the product of four fundamental design parameters (the number of both the Tx and Rx antennas, the number of RAKE fingers, and the free distance of the convolutional code) and also the fading channel parameter. Our results are sufficiently general and apply to cases where the instantaneous SNRs of the resolvable multipaths come from different Nakagami families, as well as dissimilar average SNRs from multipath components. The generality and computational efficiency of the results render themselves as powerful means for both theoretical analysis and practical applications.

REFERENCES

[1] M. Nakagami, "The m-distribution, a general formula of intensity distribution of rapid fading," in *Statistical Methods in Radio Wave Propagation*, W. G. Hoffman, Ed. Oxford, U.K.: Pergamon, 1960.

[2] P. Lombardo, D. Fedele, and M. M. Rao, "MRC performance for binary signals in Nakagami fading with general branch correlations," *IEEE Trans. Commun.*, vol. 47, pp. 44–52, Jan. 1999.

[3] M. Simon and M.-S. Alouini, "A unified approach to the performance analysis of digital communication over generalized fading channels," *Proc. IEEE*, vol. 86, pp. 1860–1877, Sept. 1998.

[4] M.-S. Alouini and A. J. Goldsmith, "A unified approach for calculating error rates of linearly modulated signals over generalized fading channels," *IEEE Trans. Commun.*, vol. 47, pp. 1324–1334, Sept. 1999.

[5] M. Z. Win, G. Chrisikos, and J. Winters, "Error probability for M-ary modulation in correlated Nakagami channels using maximal ratio combining," in *Proc. MILCOM'99*, vol. 2, Atlantic City, NJ, 1999, pp. 944–948.

[6] J. Luo, J. Zeidler, and S. McLaughlin, "Performance analysis of compact antenna arrays with MRC in correlated Nakagami fading," *IEEE Trans. Veh. Technol.*, vol. 50, pp. 267–277, Jan. 2001.

[7] T. Eng and L. B. Milstein, "Coherent DS-CDMA performance in Nakagami multipath fading," *IEEE Trans. Commun.*, vol. 43, pp. 1134–1143, Feb./Mar./Apr. 1995.

[8] G. J. Foschini and M. J. Gans, "On limits of wireless communications in a fading environment when using multiple antennas," *Wireless Personal Commun.*, vol. 6, pp. 311–335, 1998.

[9] D. Chizhik, F. Rashid-Farrokhi, and A. Lozano, "Effect of antenna separation on the capacity of BLAST in correlated channels," *IEEE Commun. Lett.*, vol. 4, pp. 337–339, Nov. 2000.

[10] K. I. Pedersen, J. B. Andersen, J. P. Kermoal, and P. Mogensen, "A stochastic multiple-input-multiple-output radio channel model for evaluation of space-time coding algorithms," *Proc. IEEE Vehicular Technology Conf. (VTC)-Fall 2000*, vol. 2, pp. 893–897, Sept. 2000.

[11] J. P. Kermoal, L. Schumacher, P. Mogensen, and K. I. Pedersen, "Experimental investigation of correlation properties of MIMO radio channels for indoor picocell scenarios," *Proc. IEEE Vehicular Technology Conf. (VTC)-Fall 2000*, vol. 1, pp. 14–21, Sept. 2000.

[12] M. Stege, J. Jelitto, M. Bronzel, and G. Fettweis, "A multiple input – multiple output channel model for simulation of Tx- and Rx-diversity wireless systems," *Proc. IEEE Vehicular Technology Conf. (VTC)-Fall 2000*, vol. 2, pp. 833–839, Sept. 2000.

[13] B. A. Bjerke, J. G. Proakis, and Z. Zvonar, "Antenna diversity combining schemes for WCDMA systems in fading multipath channels," *Proc. IEEE Vehicular Technology Conf. (VTC)-Fall 2000*, vol. 1, pp. 421–428, Sept. 2000.

[14] P. Diaz and R. Agusti, "The use of coding and diversity combining for mitigating fading effects in a DS/CDMA system," *IEEE Trans. Veh. Technol.*, vol. 47, pp. 95–102, Feb. 1998.

[15] M. K. Simon, J. K. Omura, R. A. Scholtz, and B. A. Levitt, *Spread Spectrum Communications*. Rockville, MD: Computer Sci., 1985.

[16] P. Schramm, "Tight upper bound on the bit error probability of convolutionally encoded spread spectrum communication over frequency-selective rayleigh-fading channels," *Proc. IEEE Int. Conf. Communications (ICC)'95*, vol. 3, pp. 1727–1731, June 1995.

[17] Y. F. M. Wong and K. Letaief, "Concatenated coding for DS/CDMA transmission in wireless communications," *IEEE Trans. Commun.*, vol. 48, pp. 1965–1969, Dec. 2000.

[18] C. D'Amours, M. Moher, A. Yonhacoglu, and J. Wang, "RAKE receiver structures for differential and pilot symbol-assigned detection of DS-CDMA signals in frequency-selective rayleigh fading channels," in *Proc. GLOBECOM'93*, vol. 3, Houston, TX, Dec. 1993, pp. 1798–1802.

[19] D. Nikolai, K.-D. Kammeyer, and A. Dekorsy, "On the bit error behavior of coded DS-CDMA with various modulation techniques," in *Proc. Int. Symp. Personal, Indoor, and Mobile Radio Communication (PIMRC)'98*, vol. 2, Boston, MA, Sept. 1998, pp. 784–788.

[20] F. Simpson and J. M. Holtzman, "Direct sequence CDMA power control, interleaving, and coding," *IEEE J. Select. Areas Commun.*, vol. 11, pp. 1085–1095, Sept. 1993.

[21] G. E. Corazza and R. De Gaudenzi, "Analysis of coded noncoherent transmission in DS-CDMA mobile satellite communications," *IEEE Trans. Commun.*, vol. 46, pp. 1525–1535, Nov. 1998.

[22] P. van Rooyen, "Low rate coding and diversity for cellular CDMA," *Trans. South African Inst. Elect. Eng.*, vol. 89, no. 3, pp. 113–119, Sept. 1998.

[23] R. Cideciyan, E. Eleftheriou, and M. Rupf, "Performance of convolutionally coded coherent DS-CDMA systems in multipath fading," in *Proc. GLOBECOM'96*, vol. 3, London, U.K., Nov. 1996, pp. 1755–1760.

[24] G. Femenias and I. Furio, "Dual MRC diversity reception of TCM-MPSK signals over Nakagami fading channels," *Electron. Lett.*, vol. 32, pp. 1752–1754, Sept. 1996.

[25] S. M. Alamouti, "A simple transmit diversity technique for wireless communications," *IEEE J. Select. Areas Commun.*, vol. 16, pp. 1451–1458, Oct. 1998.

[26] J. Salz and J. Winters, "Effect of fading correlation on adaptive arrays in digital mobile radio," *IEEE Trans. Veh. Technol.*, vol. 43, pp. 1049–1057, Nov. 1994.

[27] J. Fuhl, A. Molisch, and E. Bonek, "Unified channel model for mobile radio systems with smart antennas," *Proc. Inst. Elect. Eng.—Radar, Sonar, Navigat.*, vol. 145, pp. 32–42, Feb. 1998.

[28] J. G. Proakis, *Digital Communications*, 3rd ed. New York: McGraw-Hill, 1995.

[29] J. Conan, "The weight spectra of some short low-rate convolutional codes," *IEEE Trans. Commun.*, vol. 32, pp. 1050–1056, Sept. 1984.

[30] V. Tarokh, H. Jafarkhani, and A. R. Calderbank, "Space-time block codes from orthogonal designs," *IEEE Trans. Inform. Theory*, vol. 45, pp. 1456–1467, July 1999.

Jianxia Luo (S'97–M'02) received the B.Sc. degree in electronics and information systems from NanKai University, Tianjin, China, in 1992, and the M.Eng. and Ph.D. degrees, both in electrical engineering, from Jiaotong University, Shanghai, China, and University of California, San Diego, in 1995 and 2002, respectively.

Since August 1996, she has been with Hughes Network Systems, Inc., San Diego, where she was engaged in the development of Enhanced ACELP vocoder for fixed-wireless terminal and satellite-GSM dual-mode hand-held terminal. Her research interests include digital signal processing in communications, adaptive array processing, diversity reception in fading channel, and propagation aspects of mobile radio systems.

James R. Zeidler (M'76–SM'84–F'94) received the Ph.D. degree in physics from the University of Nebraska, Lincoln, in 1972.

Since 1974, he has been a scientist at the Space and Naval Warfare Systems Center, San Diego, CA. He has also been an Adjunct Professor of Electrical and Computer Engineering at the University of California, San Diego, since 1988. During this period, he has conducted research on communications systems, sonar and communications signal processing, communications signals exploitation, undersea surveillance, array processing, underwater acoustic communications, infrared image processing, and electronic devices. He was also a Technical Advisor in the Office of the Assistant Secretary of the Navy (Research, Engineering, and Systems), Washington, DC, from 1983 to 1984. He is a member of the editorial board of the *Journal of the Franklin Institute.*

Dr. Zeidler was an Associate Editor of the IEEE TRANSACTIONS ON SIGNAL PROCESSING from 1991 to 1994. He received the Lauritsen-Bennett Award for achievement in science in 2000 and the Navy Meritorious Civilian Service Award in 1991. He was a corecipient of the award for Best Unclassified Paper at the IEEE Military Communications Conference in 1995.

John G. Proakis (S'58–M'62–SM'82–F'84–LF'97) received the B.S.E.E. degree from the University of Cincinnati, Cincinnati, OH, in 1959, the M.S.E.E. degree from the Massachusetts Institute of Technology (MIT), Cambridge, MA, in 1961, and the Ph.D. degree from Harvard University, Cambridge, MA, in 1967.

He is an Adjunct Professor at the University of California, San Diego, and a Professor Emeritus at Northeastern University, Boston, MA. He was a faculty member at Northeastern University from 1969 to 1998 and held the following academic positions: Associate Professor of Electrical Engineering, 1969–1976; Professor of Electrical Engineering, 1976–1998; Associate Dean of the College of Engineering and Director of the Graduate School of Engineering, 1982–1984; Interim Dean of the College of Engineering, 1992–1993; Chairman of the Department of Electrical and Computer Engineering, 1984–1997. Prior to joining Northeastern University, he worked at GTE Laboratories, and the MIT Lincoln Laboratory. He is the author of *Digital Communications* (New York: McGraw-Hill, 1983, 1st edition; 1989, 2nd edition; and 1995, 3rd edition, 2001, 4th edition), and coauthor of *Introduction to Digital Signal Processing* (New York: Macmillan, 1988, 1st edition; 1992, 2nd edition; and 1996, 3rd edition); *Digital Signal Processing Laboratory* (Englewood Cliffs, NJ: Prentice-Hall, 1991); *Advanced Digital Signal Processing* (New York: Macmillan, 1992); *Algorithms for Statistical Signal Processing* (Englewood Cliffs, NJ: Prentice-Hall, 2002); *Discrete-Time Processing of Speech Signals* (New York: Macmillan, 1992; IEEE Press, 2000); *Communication Systems Engineering,* (Englewood Cliffs, NJ: Prentice;Hall, 1994, 1st edition, 2002 and 2nd edition); *Digital Signal Processing Using MATLAB V.4* (Boston, MA: Brooks/Cole-Thomson Learning, 1997, 2000); and *Contemporary Communication Systems Using MATLAB* (Boston, MA: Brooks/Cole-Thomson Learning, 1998, 2000). He holds five patents and has published over 150 papers. His professional experience and interests are in the general areas of digital communications and digital signal processing and, more specifically, in adaptive filtering, adaptive communication systems, and adaptive equalization techniques, communication through fading multipath channels, radar detection, signal parameter estimation, communication systems modeling and simulation, optimization techniques, and statistical analysis. He is active in research in the areas of digital communications and digital signal processing and has taught undergraduate and graduate courses in communications, circuit analysis, control systems, probability, stochastic processes, discrete systems, and digital signal processing.